Strong Field Adiabatic Ionization Prepares a Launch State for Coherent Control

ARTICLE *in* JOURNAL OF PHYSICAL CHEMISTRY LETTERS · DECEMBER 2014

Impact Factor: 7.46 · DOI: 10.1021/jz502313f

6 AUTHORS, INCLUDING:

Maryam Tarazkar
Temple University
13 PUBLICATIONS **33** CITATIONS
SEE PROFILE

Dmitri A. Romanov
Temple University
127 PUBLICATIONS **857** CITATIONS
SEE PROFILE

THE JOURNAL OF PHYSICAL CHEMISTRY Letters

Letter

pubs.acs.org/JPCL

Strong Field Adiabatic Ionization Prepares a Launch State for Coherent Control

Timothy Bohinski,[†,‡] Katharine Moore Tibbetts,[†,‡] Maryam Tarazkar,[†,‡] Dmitri A. Romanov,[‡,§] Spiridoula Matsika,[†] and Robert J. Levis*[,†,‡]

[†]Department of Chemistry, Temple University, Philadelphia, Pennsylvania 19122, United States

[‡]Center for Advanced Photonics Research, Temple University, Philadelphia, Pennsylvania 19122, United States

[§]Department of Physics, Temple University, Philadelphia, Pennsylvania 19122, United States

ABSTRACT: We demonstrate that excitation of acetophenone with a strong field, near-infrared femtosecond pulse (1150−1500 nm) results in adiabatic ionization, producing acetophenone radical cation in the ground electronic state. The time-resolved transients of the parent and fragment ions probed with a weak 790 nm pulse reveal an order of magnitude enhancement of the peak-to-peak amplitude oscillations, ∼ 100 fs longer coherence time, and an order of magnitude increase in the ratio of parent to fragment ions in comparison with nonadiabatic ionization with a strong field 790 nm pulse. Equation of motion coupled cluster and classical wavepacket trajectory calculations support the mechanism wherein the probe pulse excites a wavepacket on the ground surface D_0 to the excited D_2 surface at a delay of 325 fs, resulting in dissociation to the benzoyl ion. Direct population transfer to the D_2 state within the duration of a 1370 nm pump pulse eliminates wavepacket oscillation on the D_0 state.

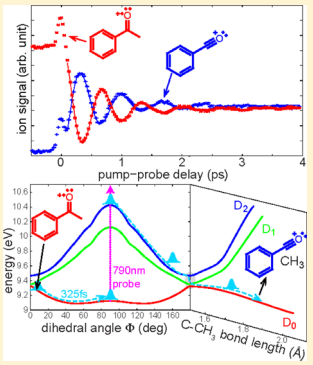

SECTION: Spectroscopy, Photochemistry, and Excited States

Although strong field ionization has revealed many novel phenomena, including high harmonic generation[1,2] and nonadiabatic multielectron excitation,[3−5] the preparation of a well-defined initial state with respect to nuclear modes in polyatomic molecules is problematic due to competing dissociation processes. In the semiclassical picture of strong-field ionization,[6] the interplay of the laser period and the electronic period controls the degree of energy transfer from the field to the outgoing electron. The same interplay should control the degree of excitation of the internal electronic degrees of freedom of the resulting ion, determining the extent of energy transfer from the electronic coordinates to the nuclear coordinates.[7] In atoms, the ionization mechanism is determined by the Keldysh adiabaticity parameter γ, where $\gamma < 1$ implies tunnel ionization and $\gamma > 1$ implies multiphoton ionization.[8] In polyatomic molecules, we propose that limited energy transfer in the adiabatic tunneling regime prepares predominantly ground state molecular ion, whereas the nonadiabatic multiphoton regime transfers energy into excited electronic states of the ion that can couple to the nuclear degrees of freedom.[5] The production of multiple initial states confounds quantum control experiments with 800 nm excitation presumably because multiple dissociation channels are accessible. This circumstance typically limits the achievable dynamic range to a factor of ∼2−4.[9−12]

In contrast, adiabatic ionization of polyatomic molecules using longer excitation wavelengths is expected to prepare a ground state molecular ion that can be used as a "launch state" for coherent control in the strong-field regime coupled to mass spectrometric detection.[3,4] This prediction has been borne out in dissociation measurements as a function of excitation wavelength in multiple molecular families.[3,4,13−19] Recent strong field experiments on acetophenone derivatives suggest that the mechanism of energy transfer from electronic to nuclear modes involves propagation of the impulsively prepared, torsional nuclear wavepacket on an excited electronic energy surface of the ion, which passes through a region of conical intersection. The resulting excess vibrational energy initiates dissociation.[17−20] These experiments show that such dissociative processes can be avoided by initially exciting the electronic degrees of freedom adiabatically, wherein no energy is transferred beyond that required for ionization.[4] To test our hypothesis that adiabatic ionization selectively produces ground-state ions, we investigate the time-resolved fragmentation response of the acetophenone radical cation using strong field pump wavelengths from 790−1500 nm and a weak-field, 790 nm, time-delayed probe. Such time-resolved experiments have revealed insight into the dissociation dynamics of many polyatomic molecules.[21−30] Acetophenone is an ideal polyatomic system because the formation of multiple fragmentation products enables determination of the populated excited states, whereas diatomics would not permit such an experiment. The mass fragments, therefore, provide an experimental observable

Received: October 31, 2014
Accepted: December 1, 2014

   dx.doi.org/10.1021/jz502313f | J. Phys. Chem. Lett. 2014, 5, 4305−4309

of the evolution of the excited state population, which may facilitate quantum control experiments.[10,26]

Ionizing pump pulses (40 μJ, 5×10^{13} W cm^{-2}, 70 ± 5 fs) are obtained from the output of a regenerative amplifier (790 nm) or an optical parametric amplifier (OPA) producing tunable near-IR pulses (1150−1550 nm). Wavepacket dynamics are probed with a weak 790 nm pulse (nonionizing, 3−5 μJ, 2×10^{12} W cm^{-2}, 60 ± 5 fs). The pump−probe time delay is scanned with a translational stage in steps of 25 fs. Both beams are focused collinearly into a vacuum chamber containing acetophenone (Sigma-Aldrich) at a pressure of 4×10^{-6} Torr. Time-of-flight mass spectra are collected on a LeCroy-LT372 oscilloscope. The absolute laser intensity and zero time delay are determined by the Xe^+ signal of added xenon gas.[31]

Figure 1a displays the parent molecular ion signal as a function of pump−probe delay for representative pump

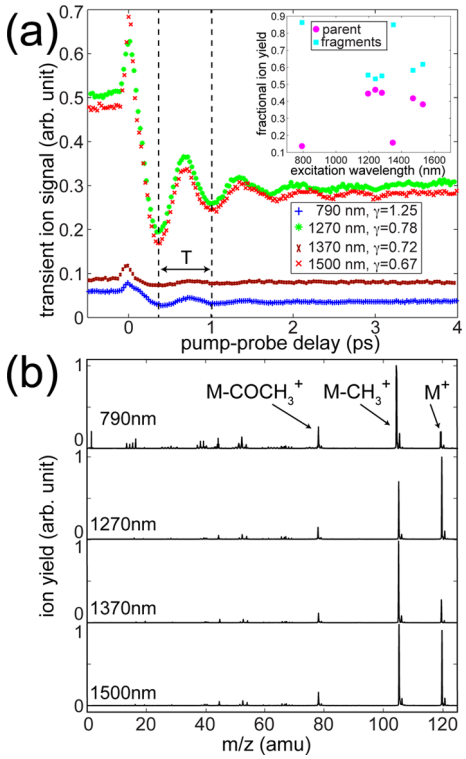

Figure 1. (a) Depicts the parent ion signal as a function of pump−probe delay for pump wavelengths of 790 nm (blue +), 1270 nm (green *), 1370 nm (maroon ×), and 1500 nm (red ×). The Keldysh parameter at each pump wavelength is listed in the legend. Dashed lines denote minima of the ion yield with a period T = 650 fs. Inset: Parent (magenta ○) and fragment (cyan □) ion signals as a function of excitation wavelength with only the pump pulse. (b) Mass spectra of acetophenone at negative time delays with pump wavelengths of 790, 1270, 1370, and 1500 nm. The parent ion (M^+), benzoyl ion (M−CH3$^+$), and phenyl ion (M−COCH3$^+$) are indicated.

wavelengths 790 nm (blue +), 1270 nm (green *), 1370 nm (maroon ×) and 1500 nm (red ×). The sample pressure in all experiments was identical, so the raw integrated ion signals could be directly compared without further normalization. At negative time delays, only the pump pulse contributes to the ion signal because the probe pulse is too weak to ionize the molecule. At zero delay, the increased ion signal arises from the overlapping of pump and probe pulses. The zero delay feature is a direct result of the intensity increase that occurs when both pulses are spatially and temporally overlapped in the focal region. The dashed vertical lines highlight two minima in the ion yield with a period of 650 fs. The peak-to-peak amplitude of the first oscillation is a factor of 10 greater using near-IR excitation. Such large amplitude oscillations are not typical in time-resolved, strong-field, pump−probe experiments.[23−30] The small parent-ion yield and low amplitude oscillation in the case of the 790 nm pump (comparable to those observed in previous experiments on acetophenone[29,30]) are consistent with the hypothesis that dissociation is caused by population of multiple excited electronic states in the cation due to nonadiabatic excitation. Additionally, the coherence time retrieved from nonlinear least-squares fitting of the experimental data increases from 440 fs for 790 nm excitation to 570 fs for 1270 and 1500 nm excitation. The Keldysh parameters listed in Figure 1 suggest that the tunneling (adiabatic) character increases as the pump wavelength is tuned from 790 to 1500 nm. The transition from nonadiabatic to adiabatic ionization is further illustrated in the inset of Figure 1a, where the fractional yields of parent (magenta ○) and fragment (cyan □) ions are plotted as a function of excitation wavelength in the absence of the probe pulse and the raw mass spectra are given for different pump wavelengths at negative time delay (Figure 1b). The increase of the relative parent ion yield, as compared with 790 nm, by a factor of 5 in the near-IR is consistent with enhanced preparation of the ion in its ground state via adiabatic ionization. Furthermore, the mass spectrum at 790 nm clearly exhibits a higher yield of small fragments ($m/z \leq 77$) than all of the longer wavelengths, which is consistent with nonadiabatic ionization at 790 nm and adiabatic ionization at the longer wavelengths.[3]

We can test the notion that strong field near-IR excitation prepares a launch state by projecting the wavepacket onto a given final state with a probe laser. Projecting from multiple initial states is expected to result in limited-amplitude modulation for a given final state due to nonadiabatic preparation of multiple excited cation states. Projecting from a single initial state should, in contrast, lead to higher-amplitude modulation. The final states in this experiment are given by the dissociation products of acetophenone: benzoyl, phenyl, acetyl, and methyl ions.[20] The yields of the parent (red ×), benzoyl (blue +), and phenyl (green *) ions are plotted as a function of delay between the pump and probe pulses in Figure 2 for pump wavelengths of (a) 790 nm, (b) 1270 nm, and (c) 1370 nm. Excitation with a 1500 nm pump pulse produces similar behavior to 1270 nm and is not shown. The signals for the acetyl and methyl ions were too low to resolve any time-dependent oscillations. The transients were fit to exponentially decaying sinusoids (Table 1), revealing an oscillation period of ~650 fs (1.481 THz) for the parent transient. This is consistent with a torsional mode at 1.436 THz in the microwave spectrum of acetophenone involving rotation about the carbon−carbon bond joining the phenyl ring to the acetyl group.[32]

To interpret the transients shown in Figure 2, a series of calculations were performed to model the wavepacket dynamics of the acetophenone molecular ion. The dihedral angle is the main coordinate changing after the creation of the molecular ion at 0° dihedral angle, with the wave packet moving toward the energy minimum at 44°. The ground and excited state energies as a function of dihedral angle were calculated at the EOM-IP-CCSD/6-311+G(d) level of theory using QCHEM.[33] The transition dipole coupling between the ground state D_0 and the excited state D_2 as a function of dihedral angle was

dx.doi.org/10.1021/jz502313f | J. Phys. Chem. Lett. 2014, 5, 4305−4309

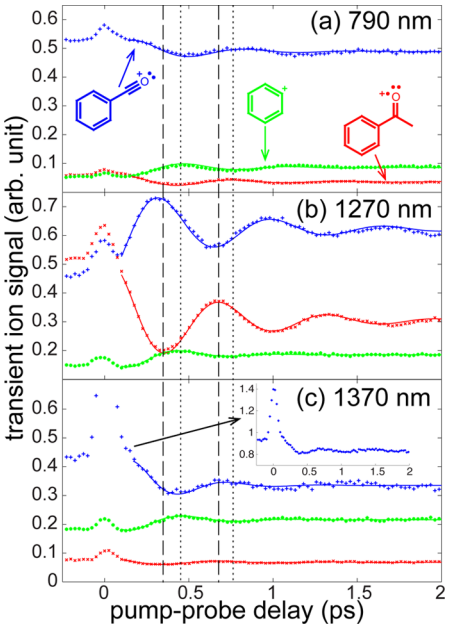

Figure 2. Time-dependent signals of acetophenone parent (red ×), benzoyl (blue +), and phenyl (green *) ions at pump wavelengths (a) 790 nm, (b) 1270 nm, and (c) 1370 nm. The solid curves are the nonlinear least-squares fits of the data to a decaying sinusoidal function. Dashed lines at 0.325 and 0.650 ps indicate the first minimum and maximum of the parent ion signal when the pump wavelength is 1270 nm. Dotted lines at 0.425 and 0.750 ps indicate the first maximum (minimum) and minimum (maximum) of phenyl (benzoyl) ion signal when the pump wavelength is 790 and 1370 nm. The inset in (c) depicts the benzoyl transient.

Table 1. Fitting Parameters for the Least Squares Curves in Figures 1 and 2[a]

ion	pump (nm)	*a*	*b* (ps)	*c* (rad)	*d* (ps)	*e*
parent	790	0.0337	0.660	0.496	0.439	0.0362
	1270	0.214	0.642	1.069	0.566	0.304
	1370	0.0146	0.664	1.324	0.542	0.083
	1500	0.280	0.660	1.026	0.540	0.332
benzoyl	790	0.0447	0.632	5.719	0.533	0.489
	1270	0.190	0.668	4.711	0.586	0.621
	1370	0.157	0.570	5.901	0.274	0.856
	1500	0.251	0.668	4.553	0.670	0.883
phenyl	790	0.027	0.614	3.733	0.603	0.0859
	1270	0.0737	0.601	2.959	0.276	0.186
	1370	0.0603	0.631	2.983	0.314	0.236
	1500	0.0585	0.608	2.927	0.366	0.147

[a]The fit equation for signal *S* as a function of time *t* (in ps) is $S(t) = a\sin((2\pi t)/b + c)\exp(t/d) + e$.

calculated at the EOM-EE-CCSD/6-31+G(d) level using Gaussian.[34] These calculations reveal a maximum dipole coupling at a dihedral angle of 90° and zero coupling at 0° and 180°. Figure 3a displays the energies of the D_0 (red ×), D_1 (green *), and D_2 (blue +) surfaces as a function of the dihedral angle with all other internal coordinates optimized. The proposed mechanism of benzoyl ion formation at the pump wavelengths of 1270 and 1500 nm is illustrated on the potential surfaces in Figure 3a. Adiabatic ionization launches a wavepacket that propagates along the D_0 surface from the initial dihedral angle of 0° toward 180°, as shown by the light blue dashed line. The D_0 to D_2 dipole coupling increases with

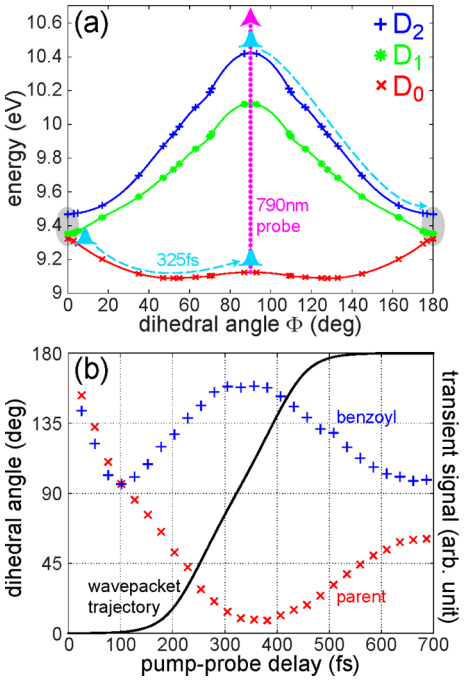

Figure 3. (a) Calculated potential energy surfaces D_0 (red ×), D_1 (green *) and D_2 (blue +) as a function of dihedral angle. The pale blue dashed lines indicate wavepacket motion on the D_0 and D_2 surfaces and the dotted line indicates the 790 nm probe photon. (b) Calculated wavepacket trajectory (black) superimposed on the parent (red ×) and benzoyl (blue +) transient signals.

increasing dihedral angle from the minimum at 0°, allowing the time-delayed probe pulse (dotted magenta arrow of length 1.6 eV) to transfer population to the D_2 surface most efficiently at a dihedral angle of 90°. Once population is transferred to the D_2 surface, the wavepacket propagates to a dihedral angle of 180° (light blue dashed line), where a conical intersection seam among $D_0/D_1/D_2$ (shaded oval) facilitates dissociation to the benzoyl ion.[17] Thus, the first maximum in the benzoyl ion yield and the concurrent minimum in the parent ion yield at a pump−probe delay of ∼325 fs correspond to the time required for the centroid of the wavepacket to reach 90°. As the dihedral angle increases past 90°, the coupling between D_0 and D_2 (and corresponding benzoyl ion yield) decreases until the minimum benzoyl/maximum parent ion yields observed at ∼650 fs, corresponding to the forbidden transition at 180°. Continued oscillation of the D_0 wavepacket produces maximum population transfer every time the dihedral angle reaches 90°, with two recurrences detectable in Figure 2b.

To test the proposed mechanism, wavepacket trajectory calculations were performed using the D_0 surface in Figure 3a. Based on the method of Zewail,[35] the evolution of the dihedral angle of the wavepacket centroid is determined by the equation of motion

$$\frac{d\varphi}{dt} = \sqrt{\frac{2}{I}(V(\varphi(0)) - V(\varphi(t)))} \quad (1)$$

where φ is the dihedral angle, I is the reduced moment of inertia for the torsional motion, and $V(\varphi(t))$ is the D_0 surface in Figure 3a. Equation 1 was solved using the numerical integrator ode45 in MATLAB, with the initial value of $\phi(0) = 10^{-4}$ radian and a reduced moment of inertia of 5.22×10^{-46} kg m^2. The calculated dihedral angle as a function of time is

dx.doi.org/10.1021/jz502313f | J. Phys. Chem. Lett. 2014, 5, 4305−4309

plotted as the thick black line in Figure 3b, along with the transient signals of the parent ion (red ×) and benzoyl ion (blue +). The trajectory calculation reveals the wavepacket reaches the geometry with largest transition probability to the dissociative D_2 state (at the dihedral angle of 90°) in approximately 320 fs, where probe−pulse excitation most effectively depletes the population on the bound D_0 state. This time delay is in agreement with the experimentally measured minimum in the parent yield and maximum in the benzoyl ion at a time delay of 325 fs. The minimum of the benzoyl ion yield and recurrence in the parent ion yield occur at 650 fs delay, in good agreement with the trajectory prediction of the calculated torsional angle reaching ∼180° at 650 fs.

The fragmentation dynamics at 1370 nm pump are distinctly different than all of the other pump wavelengths investigated in the near-IR from 1150−1500 nm. For instance, the amplitude of modulation is an order of magnitude lower than that measured at 1270 nm and the benzoyl phase changes by ∼1.2 rad (Table 1). To rationalize the 1370 nm pump transients, we consider the previously reported one-photon transition between the D_0 and D_2 surfaces of the acetophenone radical cation that occurs within the duration of the 1370 nm pulse.[20] The experiment revealed a systematic increase in the ratio of benzoyl to parent ion yields upon increasing the excitation wavelength beyond 1320 nm, which is maximized at 1370 nm. The benzoyl ion forms after wavepacket propagation on the D_2 surface reaches the conical intersection seam at 180°.[17] The transition from D_2 to D_0 provides sufficient energy on the D_0 surface to break the methyl bond and form the benzoyl ion. According to Figure 3b, the minimum of the D_0 surface at a dihedral angle of 44° (where the 1370 nm transition occurs) is reached after 250 fs of wavepacket evolution. At this time delay the temporal amplitude of the 1370 nm pump pulse (as measured by second harmonic FROG) is approximately 1% of the peak amplitude, corresponding to an intensity of 5×10^{11} W cm^{-2}. This intensity is sufficient to saturate a one-photon transition to the excited energy surface. Note that the benzoyl ion yield at zero delay for the 1370 nm pump is also a factor of 5 larger than all other experiments. This implies that the 790 nm probe contributes significantly to the D_0 initial state population, and this population is also excited to the dissociative D_2 surface by the trailing edge of the 1370 nm pump. The zero delay features for 1270, 1500, and 790 nm pump pulses are not as large because there is no one-photon transition mechanism active at these wavelengths.

The peak-to-peak amplitude of the parent-ion oscillation for the 1370 nm pump (Figure 2c) is an order of magnitude lower than that measured for 1270 nm (Figure 2b) or 1500 nm. This decrease in modulation depth supports the hypothesis that the one-photon excitation for a 1370 nm pump pulse transfers most of the D_0 wavepacket to the D_2 surface within the pump pulse duration. The marked depletion of the parent ion reflects the death of the D_0 wavepacket and the birth of a wavepacket on the D_2 surface. Another signature for the transfer of the ground-state wavepacket to the D_2 surface during the 1370 nm pump pulse is the 1.2 rad phase shift measured in the benzoyl ion transient in Figure 2c as compared with 2b (c.f., Table 1). The phase shift observed after zero delay reflects the wavepacket dynamics on the D_2 potential in comparison with D_0, which can be probed by the 790 nm pulse. Excitation to a higher lying surface, for example, D_3, by the probe pulse can result in dissociation to the phenyl ion, which accounts for the observed depletion of the benzoyl ion yield and simultaneous increase in the phenyl ion yield. The wavepacket oscillating on the D_2 surface will encounter a conical intersection that leads to depletion of the majority of the wavepacket and dissociation to form the benzoyl ion. However, a small fraction of the wavepacket remains on the D_2 surface and is subsequently excited to higher lying states, producing an additional antiphase oscillation in the phenyl and benzoyl ion transients. Under the conditions employed in the 1370 nm pump experiment, ∼ 10% of the initial wavepacket remains on the D_0 surface, as seen by the oscillations in the parent ion yield. A similar excitation path to D_2 and perhaps higher states occurs when the pump wavelength is 790 nm (Figure 2a), where limited ground ionic state population is observed and the benzoyl and phenyl transients oscillate out of phase. This circumstance indicates that excitation of acetophenone with 1370 nm results in nonadiabatic dynamics due to depletion of the D_0 wavepacket.

Time-resolved photodissociation experiments on the acetophenone radical cation revealed evidence for adiabatic ionization at 1270 and 1500 nm, where a "cold" launch state is created on the D_0 electronic surface. The corresponding antiphase oscillation of the benzoyl fragment results from population transfer from the D_0 state to the D_2 state by the 790 nm probe pulse. Elimination of the majority of the D_0 wavepacket within the duration of the 1370 nm pump pulse reveals antiphase oscillations in the benzoyl and phenyl ions, which are assigned to a secondary wavepacket oscillating on the D_2 surface with several passes through the conical intersection seam. The multiple recurrences observed suggest that adiabatic ionization enables improved manipulation of wavepackets in the vicinity of a conical intersection seam. The enhanced oscillation amplitude as compared to nonadiabatic excitation indicates a greater degree of coherence, which is advantageous for quantum control and quantum information applications.

AUTHOR INFORMATION

Corresponding Author

*E-mail: rjlevis@temple.edu.

Notes

The authors declare no competing financial interest.

ACKNOWLEDGMENTS

This work was supported by NSF grants CHE0957694 and CHE1213614.

REFERENCES

(1) Paul, P.; Toma, E.; Breger, P.; Mullot, G.; Auge, F.; Balcou, P.; Muller, H.; Agostini, P. Observation of a Train of Attosecond Pulses from High Harmonic Generation. *Science* **2001**, *292*, 1689−1692.

(2) Lewenstein, M.; Balcou, P.; Ivanov, M. Y.; L'Huillier, A.; Corkum, P. B. Theory of High-Harmonic Generation by Low-Frequency Laser Fields. *Phys. Rev. A* **1994**, *49*, 2117−2132.

(3) Lezius, M.; Blanchet, V.; Rayner, D. M.; Villeneuve, D. M.; Stolow, A.; Ivanov, M. Y. Nonadiabatic Multielectron Dynamics in Strong Field Molecular Ionization. *Phys. Rev. Lett.* **2001**, *86*, 51−54.

(4) Lezius, M.; Blanchet, V.; Ivanov, M. Y.; Stolow, A. Polyatomic Molecules in Strong Laser Fields: Nonadiabatic Multielectron Dynamics. *J. Chem. Phys.* **2002**, *117*, 1575−1588.

(5) Markevitch, A. N.; Romanov, D. A.; Smith, S. M.; Schlegel, H. B.; Ivanov, M. Y.; Levis, R. J. Sequential Nonadiabatic Excitation of Large Molecules and Ions Driven by Strong Laser Fields. *Phys. Rev. A* **2004**, *69*, 013401.

(6) Dewitt, M.; Levis, R. Concerning the Ionization of Large Polyatomic Molecules with Intense Ultrafast Lasers. *J. Chem. Phys.* **1999**, *110*, 11368−11375.

(7) Levine, R.; Bernstein, R. *Molecular Reaction Dynamics and Chemical Reactivity*; Oxford University Press: New York, 1987.
(8) Keldysh, L. Ionization in Field of a Strong Electromagnetic Wave. *Sov. Phys.—JETP* **1965**, *20*, 1307−1314.
(9) Assion, A.; Baumert, T.; Bergt, M.; Brixner, T.; Kiefer, B.; Seyfried, V.; Strehle, M.; Gerber, G. Control of Chemical Reactions by Feedback-Optimized Phase-Shaped Femtosecond Laser Pulses. *Science* **1998**, *282*, 919−922.
(10) Levis, R.; Menkir, G.; Rabitz, H. Selective Bond Dissociation and Rearrangement with Optimally Tailored, Strong-Field Laser Pulses. *Science* **2001**, *292*, 709−713.
(11) Bergt, M.; Brixner, T.; Dietl, C.; Kiefer, B.; Gerber, G. Time-Resolved Organometallic Photochemistry: Femtosecond Fragmentation and Adapative Control of CpFe(CO)2X (X = Cl, Br, I). *J. Organomet. Chem.* **2002**, *661*, 199−209.
(12) Cardoza, D.; Langhojer, F.; Trallero-Herrero, C.; Monti, O. L. A.; Weinacht, T. Changing Pulse-Shape Basis for Molecular Learning Control. *Phys. Rev. A* **2004**, *70*, 053406.
(13) Yatsuhashi, T.; Nakashima, N. Effects of Polarization of 1.4 μm Femtosecond Laser Pulses on the Formation and Fragmentation of Napthalene Molecular Ions Compared at the Same Effective Ionization Intensity. *J. Phys. Chem. A* **2005**, *109*, 9414−9418.
(14) Murakami, M.; Mizoguchi, R.; Shimada, Y.; Yatsuhashi, T.; Nakashima, N. Ionization and fragmentation of Anthracene with an Intense Femtosecond Laser Pulse at 1.4 μm. *Chem. Phys. Lett.* **2005**, *402*, 238−241.
(15) Trushin, S. A.; Fuß, W.; Schmid, W. E. Dissociative Ionization at High Laser Intensities: Importance of Resonances and Relaxation for Fragmentation. *J. Phys. B: At. Mol. Opt. Phys.* **2004**, *37*, 3897−4011.
(16) Tanaka, M.; Kawaji, M.; Yatsuhashi, T.; Nakashima, N. Ionization and Fragmentation of Alkylphenols by 0.8−1.5 μm Femtosecond Laser Pulses. *J. Phys. Chem. A* **2009**, *113*, 12056−12062.
(17) Bohinski, T.; Moore Tibbetts, K.; Tarazkar, M.; Romanov, D.; Matsika, S.; Levis, R. Measurement of Ionic Resonances in Alkyl phenyl Ketone Cations via Infrared Strong Field Mass Spectrometry. *J. Phys. Chem. A* **2013**, *117*, 12374−12381.
(18) Moore Tibbetts, K.; Bohinski, T.; Munkerup, K.; Tarazkar, M.; Levis, R. R. Controlling Dissociation of Alkyl Phenyl Ketone Radical Cations in the Strong Field Regime through Hydroxyl Substitution Position. *J. Phys. Chem. A* **2014**, *118*, 8170−8176.
(19) Bohinski, T.; Moore Tibbetts, K.; Tarazkar, M.; Romanov, D.; Matsika, S.; Levis, R. Radical Cation Spectroscopy via Tunnel Ionization. *Chem. Phys.* **2014**, *442*, 81−85.
(20) Bohinski, T.; Moore Tibbetts, K.; Tarazkar, M.; Romanov, D.; Matsika, S.; Levis, R. Measurement of an Electronic Resonance in a Ground-State, Gas-Phase Acetophenone Cation via Strong-Field Mass Spectrometry. *J. Phys. Chem. Lett.* **2013**, *4*, 1587−1591.
(21) Fuß, W.; Schmid, W. E.; Trushin, S. A. Time-Resolved Dissociative Intense-Laser Field Ionization for Probing Dynamics: Femtosecnd Photochemical Ring Opening of 1,3-Cyclohexadiene. *J. Chem. Phys.* **2000**, *112*, 8347−8362.
(22) Cardoza, D.; Pearson, B.; Weinacht, T. Dissociative Wave Packets and Dynamic Resonances. *J. Chem. Phys.* **2007**, *126*, 084308.
(23) Pearson, B.; Nichols, S.; Weinacht, T. Molecular Fragmentation Driven by Ultrafast Dynamic Ionic Resonances. *J. Chem. Phys.* **2007**, *127*, 131101.
(24) Nichols, S.; Weinacht, T.; Rozgonyi, T.; Pearson, B. Strong-Field Phase-Dependent Molecular Dissociation. *Phys. Rev. A* **2009**, *79*, 043407.
(25) Geißler, D.; Rozgonyi, T.; Gonzalez-Vazquez, J.; Gonzalez, L.; Nichols, S.; Weinacht, T. Creation of Multihole Molecular Wave Packets via Strong-Field Ionization. *Phys. Rev. A* **2010**, *82*, 011402.
(26) Geißler, D.; Marquetand, P.; Gonzalez-Vazquez, J.; Gonzalez, L.; Rozgonyi, T.; Weinacht, T. Control of Nuclear Dynamics with Strong Field Ultrashort Laser Pulses. *J. Phys. Chem. A* **2012**, *116*, 11434−11440.
(27) Ho, J.; Chen, W.; Cheng, P. Femtosecond Pump-Probe Photoionization-Photofragmentation Spectroscopy: Photoionization-Induced Twisting and Coherent Vibrational Motion of Azobenzene Cation. *J. Chem. Phys.* **2009**, *131*, 134308.
(28) Brogaard, R. Y.; Møller, K. B.; Sølling, T. I. Real-Time Probing of Structural Dynamics by Interaction between Chromophores. *J. Phys. Chem. A* **2011**, *115*, 12120−12125.
(29) Zhu, X.; Lozovoy, V.; Shah, J.; Dantus, M. Photodissociation Dynamics of Acetophenone and Its Derivatives with Intense Nonresonant Femtosecond Pulses. *J. Phys. Chem. A* **2011**, *115*, 1305−1312.
(30) Konar, A.; Shu, I.; Lozovoy, V. V.; Jackson, J. E.; Levine, B. G.; Dantus, M. Polyatomic Molecules under Intense Femtosecond Laser Irradiation. *J. Phys. Chem. A* **2014**, DOI: 10.1021/jp505498t.
(31) Hankin, S. M.; Villeneuve, D. M.; Corkum, P. B.; Rayner, D. M. Intense-Field Laser Ionization Rates in Atoms and Molecules. *Phys. Rev. A* **2001**, *64*, 013405.
(32) Durig, J.; Bist, H.; Furic, K.; Qiu, J.; Little, T. Far Infrared Spectra and Barriers to Internal Rotation of Benzaldehyde, Benzoyl Fluoride, Benzoyl Chloride and Acetophenone. *J. Mol. Struct.* **1985**, *129*, 45−56.
(33) Shao, Y.; Molnar, L.; Jung, Y.; Kussman, J.; Ochsenfeld, C.; Brown, S.; Gilbert, A.; Slipchenko, L.; Levchenko, S.; O'Neill, D.; DiStasio, R. C., Jr. Advances in Methods and Algorithms in a Modern Quantum Chemistry Program Package. *Phys. Chem. Chem. Phys.* **2006**, *8*, 3172−3191.
(34) Frisch, M.; Trucks, G.; Schlegel, H.; Scuseria, G.; Robb, M.; Cheeseman, J.; Scalmani, G.; Barone, V.; Mennucci, B.; Petersson, G. *Gaussian 09*, Revision B.01; Gaussian, Inc.: Wallingford, CT, 2009.
(35) Rose, T.; Rosker, M.; Zewail, A. Femtosecond Realtime Probing of Reactions. IV. The Reactions of Alkali Halides. *J. Chem. Phys.* **1989**, *91*, 7415−7436.